Proc. Natl. Acad. Sci. USA
Vol. 85, pp. 3338–3342, May 1988
Biochemistry

Structural principles of parallel β-barrels in proteins

(protein structure/β-sheets)

IGNACE LASTERS*, SHOSHANA J. WODAK†‡, PHILIPPE ALARD*, AND ERIC VAN CUTSEM†

*Plant Genetic Systems and †Unité de Conformation de Macromolécules Biologiques, Université Libre de Bruxelles, C.P. 160, P2, Avenue P. Héger, 1050 Brussels, Belgium

Communicated by Marc van Montagu, December 7, 1987 (received for review August 5, 1987)

ABSTRACT **Eight-stranded β-sheets in nine protein structures containing "TIM (triose phosphate isomerase) barrels" are shown to be fitted satisfactorily by hyperboloids, the generating lines of which pass through the β-strands. Simple parameterizations of the hyperboloid model are then used to determine the constraints that govern key parameters, such as the number of strands in the barrel, and to rationalize the remarkable conservation of strand number, observed to be eight, in nearly all the known examples of parallel β-barrels. It is shown that the requirement to exclude solvent from the barrel interior, while at the same time keeping an upper limit on strand twist and interstrand distance so as to foster extensive hydrogen bonding interactions within the sheet, imposes strong constraints on barrel geometry. A formal description of the relationships between β-sheet twist, strand number, and barrel dimensions is given here. It could have important implications for studies of protein folding and design.**

Analysis of known protein structures (1–3) has shown that they are often organized into smaller units called domains and that these domains display a limited repertoire of folding patterns. One such pattern is the eight-stranded parallel β-barrel, found to occur in proteins of the α/β class.

First observed in triose phosphate isomerase (4) and therefore called the "TIM barrel," it has since been found in one domain of pyruvate kinase (5), in aldolase (6), taka-amylase (7), and more recently in other proteins: glycolate oxidase (8), ribulose-1,5-bisphosphate carboxylase (9), cytochrome b_2 (24), trimethanol aminedehydrogenase (25), muconate lactonizing enzyme (10), xylose isomerase (11), and phosphoribosyl-anthranilate isomerase indoleglycerol phosphate synthase (12). These proteins display no sequence homology and perform different enzymatic reactions on a variety of substrates. This suggests that the parallel β-barrel is a stable building block onto which different functionalities can be designed.

Detailed descriptions of β-sheet topologies (13, 14), aligned β-sheet packing (15, 16), and orthogonal β-sheet packing (17) have been published. Parallel β-barrels were either not considered or only briefly studied since very few examples were known.

In the present study, we reparametrize a simple hyperboloid model—previously shown to yield a good description of the TIM barrel (18)—to analyze a larger data base of eight-stranded parallel β-barrels, including a total of nine structures.

We confirm that the principal features of the parallel β-barrels arise from the right-handed twist of the β-sheet that forms a closed uniformly distorted surface, which is adequately described by the hyperboloid model in all the proteins we analyzed. The relative orientation of β-sheets across the barrel is orthogonal, but contacts between sheets are generally weaker than in orthogonal packing of anti-parallel sheets (17).

Next, calculations on model hyperboloids are performed to establish the relationship between strand number and other key parameters of the β barrel, and constraints that govern these parameters are determined.

Fitting Hyperboloids to Observed Parallel β-Barrels

Table 1 lists the nine structures analyzed in this study. Atomic coordinates were taken from the Protein Data Bank (19) or were obtained from the authors.

Hyperboloids defined by the quadratic equation $(x/a)^2 + (y/b)^2 - (z/c)^2 = 1$ are fitted to the β-sheets by using the procedure described in the legend of Table 1.

Fig. 1 illustrates the fit obtained for the barrel in TIM. It is typical of the results obtained with the other eight barrels summarized in Table 1. rms distances of C_α positions to the least-squares lines in individual β-strands are found to be 1.0 Å on the average, suggesting that the strands in our sample display, in general, only a minimal amount of coil (20). The equatorial planes of the hyperboloids cut through the β-sheets. Intersection points of strand axes with the equatorial plane in each barrel are, in general, very close to intersection points of the generating lines, with an average deviation of only 0.27 Å, as illustrated in Fig. 2. However, the fit between β-strands and generating lines becomes less perfect further away from the equator. It remains nevertheless acceptable for the purpose of our analysis since the average deviation of a β-strand axis from the orientation of a generating line $\langle\theta\rangle$ is small (5°–9°), and comparable to the standard deviations of relevant angular parameters such as T_z, or the interstrand twist (see below).

A better approximation to the barrel surfaces could undoubtedly be obtained with a more sophisticated model, such as the twisted hyperboloid (18). But such a model would not be as conveniently expressed in terms of strand number or twist as its simpler variant used here.

Geometric Properties of Parallel β-Barrels

Table 1 lists the relevant geometrical parameters for each of the nine barrels analyzed.

The average angle made by β-strand axes with the barrel axis $\langle T_z\rangle$ equals 36° and is virtually invariant among barrels. The c parameter is also very similar in different proteins, whereas significant variability occurs in the lengths of the semiaxes a and b. Consequently, the barrel axial ratios $l = a/b$ vary by as much as 40%, corresponding to a wide range of equatorial shapes: the barrels in cytochrome b_2 and indolglycerol phosphate synthase are nearly circular with $l = 1.04$, and $l = 1.0$, respectively, whereas that of TIM is elliptical with $l = 1.48$. On the other hand, areas of the

The publication costs of this article were defrayed in part by page charge payment. This article must therefore be hereby marked "*advertisement*" in accordance with 18 U.S.C. §1734 solely to indicate this fact.

Abbreviation: TIM, triose phosphate isomerase.

‡To whom reprint requests should be addressed.

Table 1. Geometric parameters of parallel β-barrels

	a, Å	*b*, Å	*c*, Å	*A*, Å²	⟨*D*⟩, Å	⟨T_z⟩, degrees	⟨T_w⟩, degrees	⟨θ⟩, degrees
TIM	8.3	5.6	10.2	146	4.4 (0.4)	−35 (5)	−25 (11)	5.2 (2)
TAA	7.5	6.7	10.0	158	4.2 (0.2)	−37 (8)	−28 (6)	8.7 (2)
GLO	7.5	6.6	9.8	155	4.2 (0.6)	−36 (4)	−26 (11)	8.5 (4)
TMADH	8.4	6.4	11.1	170	4.7 (0.5)	−35 (4)	−25 (9)	5.6 (4)
B2C	7.5	7.2	10.1	169	4.6 (0.4)	−37 (5)	−27 (5)	5.2 (3)
PYK	8.6	7.2	11.3	195	5.0 (0.5)	−36 (5)	−27 (7)	6.6 (2)
KGA	8.1	6.4	10.2	163	4.4 (0.9)	−36 (6)	−26 (15)	8.2 (4)
IGPS	7.1	7.1	11.2	158	4.4 (0.4)	−34 (8)	−25 (6)	9.6 (3)
PRAI	7.4	6.4	10.7	149	4.4 (0.3)	−33 (4)	−24 (6)	4.8 (2)

TIM, triose phosphate isomerase; TAA, taka-amylase; GLO, glycolate-oxidase; TMADH, trimethanolamine dehydrogenase; B2C, cytochrome b_2; PYK, pyruvate kinase; KGA, aldolase; IGPS, indolglycerol phosphate synthase; PRAI, phosphoribosylanthranilate isomerase domain 1 and domain 2. *a*, *b*, and *c* are, respectively, the major and minor semiaxes and the curvature along the *z* axis of the fitted hyperboloid; *A*, equatorial surface; ⟨*D*⟩, average distance between axes of adjacent β-strands; ⟨T_z⟩, average angle between β-strand axes and the *z* axis of the fitted hyperboloid; ⟨T_w⟩, average twist angle between axes of adjacent β-strands; ⟨θ⟩, average deviation between axes of β-strands from the expected orientation of the corresponding generating lines of a hyperboloid of revolution. Standard deviations of *D*, T_z, T_w, and θ are in parentheses. The hyperboloids are fitted as follows: Limits of β-strands belonging to a given β-barrel are determined (see below). Least-squares lines are fitted to the C_α atoms of each strand. Direction cosines of the hyperboloid axis are determined by averaging the direction cosines of the β-strand axes in the barrel. Next, the position of the equatorial plane is obtained by an iterative procedure, and the intersection points of β-strand axes with this plane are computed. The geometric center of the intersection points of strand axes with the equatorial plane defines the hyperboloid center. A simple least-squares analysis of the same points is used to compute the directions and lengths of the major and minor semiaxes. Finally, the *c* parameter of the hyperboloid is computed by the following expression as a function of α, the angular coordinate in the equatorial plane, and T_z: $c = \cot(T_z)\cdot[a^2\cdot\sin^2\alpha + b^2\cdot\cos^2\alpha]^{0.5}$. The position of the equatorial plane is determined by an iterative procedure: a plane perpendicular to the hyperboloid axis is positioned to minimize the distance between the intersection points of β-strand axes and the hyperboloid center. Residue limits of β-strands a–h in the barrels analyzed are as follows: TIM: a, 6–12; b, 38–42; c, 60–63; d, 89–93; e, 122–129; f, 159–167; g, 205–209; h, 227–231. TAA: a, 10–15; b, 58–64; c, 112–118; d, 202–206; e, 226–231; f, 248–252; g, 289–293; h, 323–329. GLO: a, 73–76; b, 101–105; c, 124–128; d, 151–155; e, 220–223; f, 241–245; g, 275–278; h, 297–301. TMADH: a, 23–26; b, 54–58; c, 98–101; d, 165–169; e, 219–224; f, 254–257; g, 295–299; h, 320–323. B2C: a, 191–194; b, 224–227; c, 250–253; d, 276–279; e, 345–348; f, 367–370; g, 405–410; h, 428–433. PYK: a, 4–10; b, 25–29; c, 60–65; d, 172–178; e, 197–202; f, 218–222; g, 246–250; h, 279–283. KGA: a, 29–34; b, 57–61; c, 79–82; d, 101–105; e, 118–121; f, 139–142; g, 168–171; h, 193–196. IGPS: a, 49–54; b, 81–86; c, 112–116; d, 137–141; e, 159–164; f, 180–184; g, 210–215; h, 232–236. PRAI: a, 256–261; b, 278–281; c, 306–311; d, 330–334; e, 354–359; f, 377–381; g, 402–406; h, 423–426.

equatorial cross sections, computed by using the expression $A = \pi a\cdot b$, remain rather constant, with a mean value of 163 Å², and a standard deviation of ≈10%.

For each barrel, we also compute the average distance ⟨*D*⟩ between axes of adjacent β-strands and the average angle between these axes (the twist angle) ⟨T_w⟩. Both parameters, which are independent of the hyperboloid fit, vary little among barrels. In all 72 pairs of adjacent β-strands in our sample, ⟨*D*⟩ has a mean of 4.5 Å and a standard deviation of 0.34 Å, and ⟨T_w⟩ has a mean of −26° and a standard deviation of only 8°. By way of comparison, the distribution of twist angles in anti-parallel β-sheets has a mean of −24° and a standard deviation of 17° (17). The latter is nearly twice as large as in the sample analyzed here, confirming earlier observations by Salemme *et al.* (13, 14) that the surfaces of β-sheets formed by parallel β-strands are more regular than surfaces of β-sheets formed by anti-parallel strands. Moreover, our analysis clearly indicates that earlier conclusions by Chothia and Janin (17), based on the study of anti-parallel β-sheets and stating that barrels cannot be readily formed by the uniform distortion of a regular sheet, do not apply to the type of structures analyzed here.

Sheet Packing in Parallel β-Barrels

Since the axis of a regular hyperboloid is also a symmetry axis, any portion of the β-sheet surface may be generated from another by a 2-fold rotation about this axis. The angle between sheets therefore assumes the value $\Omega = 2\langle T_z\rangle$. With values of ⟨$T_z$⟩ of −36° as obtained in our barrel sample, Ω is −72°, corresponding to orthogonal sheet packing (17).

To evaluate the contributions of sheet–sheet interactions to the observed barrel structures, a more detailed analysis of sheet packing is carried out on six β-barrels, where positions for side-chain atoms were available: TIM, taka-amylase, glycolate-oxidase, aldolase, indolglycerol phosphate synthase, phosphoribosyl-anthranilate isomerase. In each case, interactions between different β-sheet pairs, corresponding to circular permutations of four adjacent β-strands, are evaluated quantitatively.

The procedure consists in computing, for each β-sheet pair, a quantity termed the "Van der Waals contact area," by using an analytic algorithm (P.A., unpublished data). This quantity is obtained by summation of contact areas of individual atom pairs (computed in the presence of β-sheet residues only), where each member of the pair belongs to a different sheet. For a given pair of atoms the contact area is defined as the portion of the circular cross section formed by their interpenetrating Van der Waals radii (also called the radical plane) that is not masked by radical planes formed with neighboring atoms. Care is taken not to include contacts between adjacent β-strands in the computations.

In TIM, consistent with its high axial ratio (l = 1.48), one β-sheet pair, composed of strands defg and habc, interacts more extensively (contact area of 68 Å²). In the other five barrels, whose cross sections are more circular, contact areas between sheets are significantly smaller (the largest area is 53 Å² for the defg/habc pair in aldolase) with little or no packing preference for any given pair of sheets.

For comparison, contact areas between several anti-parallel sheets exhibiting orthogonal packing are computed by the same procedure by using published coordinates (19) and sheet definitions (17). Intersheet contact areas in alcohol dehydrogenase and tosyl-elastase (respectively, 149 and 132 Å²) are about twice as large as the largest contact area between sheets computed in our sample, along the minor axis in TIM, whereas in *Staphylococcus* nuclease, sheet packing is less extensive (90 Å²), but still tighter than in TIM.

Weaker interactions in orthogonally packed parallel versus anti-parallel sheets may have multiple origins: larger separations between sheets, less strand coiling, difference in amino acid composition, or simply lesser accuracy of the atomic coordinates of the protein sample studied here. Data from a larger sample of refined barrel structures are needed to evaluate contributions from each of these effects.

Our preliminary results indicate that, except for TIM, sheet separations in all six β-barrels analyzed are consistently larger (11.6–13 Å) than those computed by the same procedure in orthogonal packing of anti-parallel sheets (8.5–11.5 Å) (17).

On the other hand, comparison of residue composition in our barrel sample with that found in anti-parallel β-sheet packing (ref. 18; unpublished data) indicates no significant differences. Yet, a closer examination of sheet packing in TIM suggests that an influence from amino acid composition

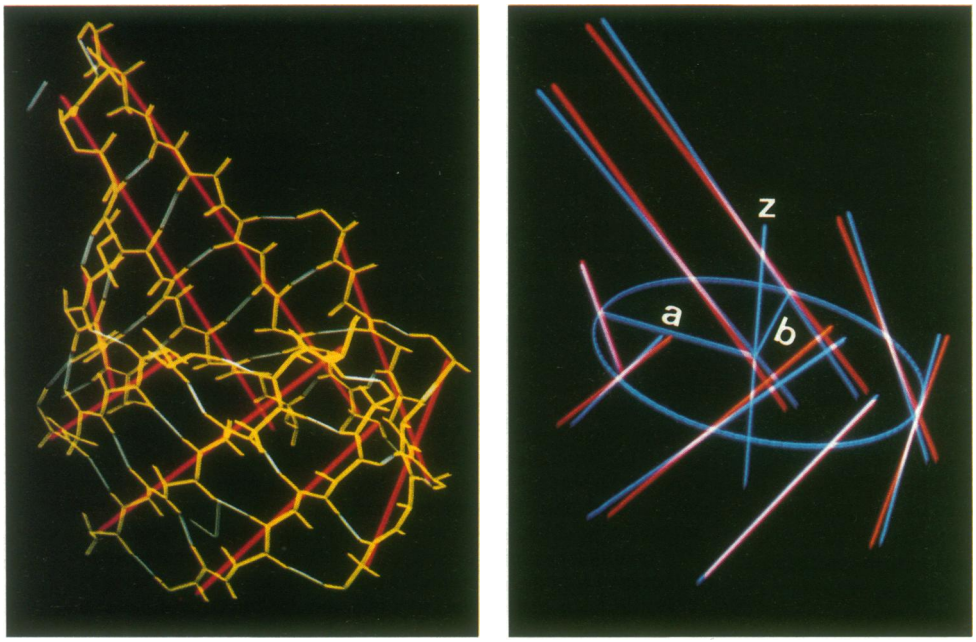

FIG. 1. Fit of a regular hyperboloid to the β-sheet portion in TIM. (*Left*) Main chain of β-strands in TIM (yellow) and computed least-squares axes (red). H bonds between strands are drawn in white. Limits of β-strands are listed in legend of Table 1. (*Right*) Deviations of β-strand axes (red) from the expected orientations of corresponding generating lines (blue) for TIM. The hyperboloid equatorial cross section, major (a) and minor (b) semiaxes as well as the hyperboloid axis (Z), are drawn in blue.

exists. The TIM barrel has a large cavity in its center (21), lined by small residues Ala-62 and Gly-9. This cavity will account at least in part (unpublished results) for the smaller contact area in TIM relative to *Staphylococcus* nuclease, where intersheet distance is 11.4 Å, compared to 10.1 Å in TIM.

Constraints That Govern the Topology of Regular Barrels

In this section, the hyperboloid equations are reparameterized to establish the relationship between strand number and other key parameters of the β-barrels, and constraints that determine the topology of these structures are analyzed.

To simplify the mathematical formalism, we consider a circular hyperboloid. The parameters needed to describe it analytically are $a = b = R$ and c, with R being the radius of the equatorial cross section. These parameters can be readily expressed in terms of the distance D and the twist angle T_w between two adjacent regularly spaced generating lines, and the number N of generating lines by the following equations:

$$c^2 = D^2[\cos(T_w) + 1] / \{4\,[1 - \cos(T_w)]\} \quad [1]$$

$$R^2 = c^2[1 - \cos(T_w)] / [\cos(T_w) - \cos\alpha], \quad [2]$$

where $\alpha = 2\pi/N$ is the angular spacing between two adjacent generating lines.

Thus, given T_w, D, and N, the hyperboloid is fully determined.

Our analysis shows all three parameters to be highly conserved in the barrels we studied, suggesting that important constraints may be involved. The interstrand distance D is

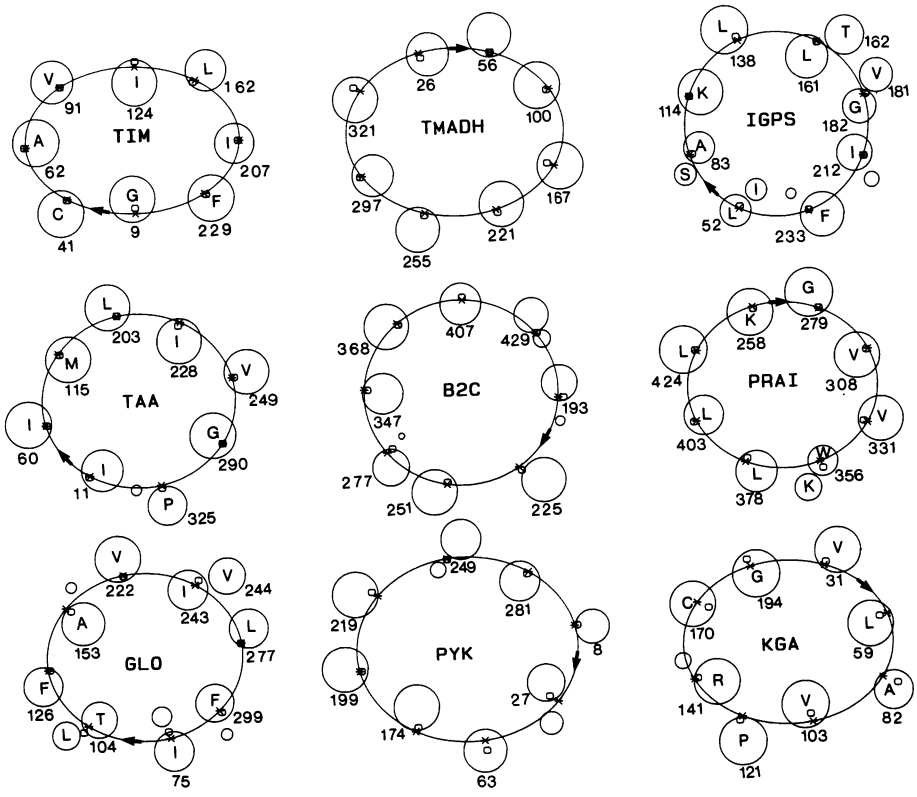

FIG. 2. Equatorial cross sections of parallel β-barrels from six proteins. Intersection points of least-squares lines passing through β-strands (○) and of generating lines in fitted hyperboloids (×) are shown. N termini of β-strands are directed toward the viewer and arrows always pointing from the first to the second β-strands indicate arrangement of strands in the barrels. Large circles represent cross sections produced by the equatorial plane cutting through the Van der Waals spheres of all the barrel C_α atoms. These atoms are marked by their sequence number and, whenever possible, by the one-letter amino acid code. See Table 1 for enzyme abbreviations.

unquestionably the most strictly constrained parameter—it must remain around 4.5 ± 1 Å to allow for H bonds to form between strands—whereas the constraints operating on the twist angle T_w and the strand number N are less obvious.

To examine this question, Eqs. 1 and 2 are solved keeping D fixed at 4.5 Å and using three different values of T_w—−26°, −40°, and −60°. For each of these values, N is varied systematically in the range that yields real solutions of the quadratic hyperboloid equations. Parameters of the computed hyperboloids are listed in Table 2.

Relationship Between Strand Number and Twist Angle. Clearly evident from Table 2 is the strong interdependence of the twist angle T_w and the strand number N. When T_w = −26°, the observed value in our barrel sample, a rather wide range of N (from 4 to 12) yields solutions to the hyperboloid equation (Table 2, Exp. a). This range is markedly reduced in hyperboloids with higher twist angles: N ranges from 4 to 8 for hyperboloids with T_w = −40°, and only from 4 to 5 for T_w = −60° (Table 2, Exps. b and c). We see, however, that computed hyperboloids span a wider range in N than real β-barrels. This is verified especially for hyperboloids with T_w = −26° and suggests that constraints due to the physical nature of proteins may be at play to further reduce the allowed range in N.

Requirement for Optimal Packing Inside the Barrel. It is reasonable to assume that a stable barrel structure will exclude bulk solvent from the interior and display favorable, mostly intramolecular, packing interactions. We suggest that this cannot be achieved by hyperboloids with $N < 5$ or > 8.

Table 2. Geometric parameters of computed circular hyperboloids

N	R, Å	Ω, degrees	A, Å²	S
	Exp. a: D = 4.5 Å, T_w = −26°			
4	3.3	−37	34	1.9
5	4.0	−45	51	2.9
6	4.9	−53	76	4.2
7	5.9	−63	110	5.9
8	7.1	−72	158	8.0
9	8.5	−82	229	10.9
10	10.3	−93	338	14.7
11	12.9	−106	527	20.2
12	17.1	−121	926	29.2
	Exp. b: D = 4.5 Å, T_w = −40°			
4	3.4	−58	37	3.1
5	4.5	−71	62	4.9
6	5.8	−86	106	7.8
7	7.9	−104	198	12.4
8	12.3	−127	479	22.1
	Exp. c: D = 4.5 Å, T_w = −60°			
4	3.9	−90	48	5.5
5	6.3	−117	125	11.2

Geometric parameters of circular hyperboloids computed by using a fixed distance D = 4.5 Å and three different twist angles T_w (Exps. a–c). For each twist angle, listed parameters correspond to all real solutions of Eqs. 1 and 2. N, number of strands in hyperboloid. R, hyperboloid radius in Å. Ω, angle between β-strand axes across the hyperboloid, computed as $2 \times T_z$, with $T_z = \arccos[c/(c^2 + R^2)^{1/2}]$ being the angle of a generating line (or β-strand axis) with the hyperboloid axis, and c is as explained in the text. A, equatorial cross section in Å². S, shear number (22) is computed by using the expression $S = N[(D/a)\tan(T_z)]$, where a is the distance between adjacent C_α atoms in a β-strand projected along its axis, and other parameters are as defined above. Note that intersheet distance estimated from the value of the hyperboloid radius R (intersheet distance = $2R$) will be overestimated by ≈1 Å compared to values cited in the literature that represent distances between the geometric centers of two sheets.

Hyperboloids with $N < 5$ are too narrow to accommodate proper packing inside the barrel, since their cross sections are narrower (8 Å or less) than the shortest distance between sheets encountered in proteins (18). On the other hand, hyperboloids with more than eight strands have cross sections of 16 Å or more and are therefore wider than the widest hyperboloid in our protein sample. Intersheet distance in the corresponding barrels is therefore too large to foster contacts, and the barrel interior may become accessible to solvent. This should be energetically unfavorable, at least as long as the barrel interior is hydrophobic.

The effect of N on the dimensions of the barrel interior is dramatically emphasized by its influence on A, the area of the equatorial cross section (Table 2). In hyperboloids with T_w = −26°, each additional strand in the barrel corresponds to a 50% increase in A, while in those with T_w = −60° (Table 2, Exp. c), going from four to five strands will nearly triple this area.

Moreover, only very few hyperboloids in Table 2 have values of A that fall within 25% of the average of 163 Å², computed in our protein sample. It is satisfying to see that, for T_w = −26°, only hyperboloids with eight strands have A values in this range. For larger twist angles, T_w −40° and −60°, our model predicts that barrels with, respectively, seven and five strands should have acceptable values of A.

This prediction seems to be borne out at least in part. Indeed, the five-stranded barrel in Table 2, Exp. c (T_w = −60°) closely resembles the parallel β-barrel formed around the 5-fold axis by the N-terminal part of the VP3 domains in the rhinovirus structure (23). Using published coordinates (19) and the procedure described above, we determine the following parameters for this barrel: T_w = −63°, R = 5.97 Å, D = 3.8 Å, and T_z = −62°. These values are in very good agreement with our predictions.

It is worthwhile to add that, as a result of the large twist angle between strands in this structure and the limited amount of strand coil, fewer interstrand H bonds are formed (only one or two, as compared to five or more in our barrel sample) and the barrel is much more open, with c values around 3 rather than 10 as in the eight-stranded barrels computed with T_w = −26°. Our calculations suggest that barrels with intermediate twist angles (e.g., −40°) should display intermediate characteristics.

Other Constraints. We have seen in the preceding sections that the mathematical constraints imposed by the hyperboloid equations and the requirement for optimal packing inside the barrel are sufficient to explain the properties of observed parallel β-barrels. Other factors, such as the angle between sheets across the barrel (Ω) or maintaining a regular arrangement of residues on the barrel surface [a property described by the shear number S (22)], are therefore bound to be of lesser consequence. Indeed, we see (Table 2) that Ω increases with increasing N in circular hyperboloids computed with constant D and T_w, and that it spans a wide range of values (−40° to −127°), all of which have been observed in proteins in either aligned or orthogonal sheet packing. The role of the shear number S is harder to assess in the framework of our model. S must have even parity for a hyperboloid whose surface is made of a regular β-sheet (22). We find that only specific values of N correspond to an even shear number in the circular hyperboloids (Table 2). But since the parity of S is very sensitive to values of other geometric parameters, such as interstrand distance, only qualitative conclusions can be drawn.

We have so far considered only circular hyperboloids. It may be argued therefore that barrels with $N > 8$ could still comply with packing requirements by deviating from a circular shape, in particular since we observe axial ratios of up to 1.48 in our barrel sample.

This question has been briefly addressed by extending our analysis to hyperboloids with elliptical cross section.

We find that the variance in T_w increases drastically with increasing axial ratio: with $N = 10$ and an axial ratio of 3, $T_w = -26.3° \pm 20°$. Highly elliptical barrels will therefore have very twisted corners and be more like double layers of orthogonally packed β-sheets (values of Ω remain between $-70°$ and $-110°$), resembling orthogonal arrangements found in anti-parallel sheets, except that, in the latter case, the highly twisted corners are achieved through a right angle bend of a long β-strand (17) that provides a covalent link between layers, while in the parallel case such a link cannot occur.

Discussion

Parameters that govern parallel β-barrel structures in proteins have been analyzed in the context of a model of a regular hyperboloid. The features of these structures are shown to arise primarily from two factors: the right-handed twist of the β-sheet, which governs both the topology of the β-sheet surface and its stability through interstrand H bonds, and from the requirement to exclude solvent from the barrel interior, which puts severe constraints on barrel dimensions.

Barrels that make up the protein core, as in the nine enzyme structures analyzed here, appear to tolerate little variability in these two major factors, resulting in a remarkable conservation of key geometric parameters, such as interstrand twist and the strand number ($N = 8$). Our analysis suggests that these barrels represent optimal solutions to the problem of forming regular hyperboloids from a β-sheet. In agreement with this hypothesis is the following observation. Adjacent C_α atoms in neighboring strands lying near or at the equatorial plane, where the surface curvature is highest, point alternatively inside and outside the barrel, as illustrated in Fig. 2. This corresponds to a situation of optimal side-chain packing and is a direct consequence of the value of one key parameter: the orientation of strand axes relative to the barrel T_z, which in turn depends on the strand twist T_w. Barrels with T_z significantly different from the values computed in our barrel sample and in the seven- or eight-stranded circular barrels of Table 2, Exp. a will deviate from this ideal packing arrangement and possibly result in less stable structures.

Our study also predicts the existence of other optimal barrel structures with higher twist angles and fewer strands. One of these, a five-stranded parallel β-barrel, actually occurs in the rhinovirus structure. It is interesting to note that this barrel is formed by the N-terminal ends of five different polypeptide chains belonging to the VP3 domains and that it has few H bonds between strands and a high proportion of proline residues.

While further analysis is clearly needed to confirm our suggestions, our study provides a formal description of the relationships between β-sheet twist, strand number, and barrel dimensions that could serve as useful guidelines in studies of protein folding and design.

The large sequence variability in our protein sample suggests that the geometric and physical constraints that govern these structures can be satisfied by many different amino acid sequences. Understanding the role played by the amino acid sequence in determining the observed structures and their biological function clearly remains a major challenge.

We thank Drs. C. Brändén, H. Jansonius, S. Matthews, D. C. Phillips, and A. Tulinsky for the gift of atomic coordinates; M. Claessens for helpful discussions; and M. Bardiaux, Ph. Delhaise, and M. de Maeyer for help in using the BRUGEL package. We are grateful to Dr. M. Rossmann for attracting our attention to the barrel in the rhinovirus structure.

1. Richardson, J. S. (1981) *Adv. Protein Chem.* **34,** 167–339.
2. Janin, J. & Wodak, S. (1985) *Prog. Biophys. Mol. Biol.* **42,** 21–78.
3. Levitt, M. & Chothia, C. (1976) *Nature (London)* **261,** 552–557.
4. Banner, D. W., Bloomer, H. C., Petsko, G. A., Phillips, D. C., Pogson, C. I. & Wilson, A. I. (1975) *Nature (London)* **255,** 609–614.
5. Stuart, D. I., Levine, M., Muirhead, H. & Stammers, D. K. (1979) *J. Mol. Biol.* **134,** 109–142.
6. Mavridis, I. M., Hatada, M. H., Tulinsky, A. & Lebioda, L. (1982) *J. Mol. Biol.* **162,** 419–444.
7. Matsuura, Y., Kusunoki, M., Harada, W., Tanaka, N., Iga, Y., Yasuoka, N., Toda, H., Narita, K. & Kakudo, M. (1980) *J. Biochem.* **87,** 1555–1558.
8. Lindqvist, Y. & Brändén, C. I. (1985) *Proc. Natl. Acad. Sci. USA* **82,** 6855–6859.
9. Schneider, G., Lindqvist, Y., Andersson, I., Knight, S., Brändén, C. I. & Lorimer, G. (1986) *EMBO J.* **5,** 3409–3415.
10. Goldman, A., Ollis, D. L. & Steitz, T. (1987) *J. Mol. Biol.* **194,** 143–153.
11. Carrel, H. L., Rubin, B. H., Hurley, T. J. & Glusker, J. P. (1984) *J. Biol. Chem.* **259,** 3230–3236.
12. Priestle, J. P., Grutter, M. G., White, J. L., Vincent, M. G., Kania, M., Wilson, E., Jardetzky, T. S., Kirschner, K. & Jansonius, J. N. (1987) *Proc. Natl. Acad. Sci. USA* **84,** 5690–5694.
13. Salemme, F. R. & Weatherford, D. W. (1981) *J. Mol. Biol.* **146,** 101–117.
14. Salemme, F. R. (1983) *Prog. Biophys. Mol. Biol.* **42,** 95–133.
15. Cohen, F. E., Sternberg, M. J. E. & Taylor, W. R. (1981) *J. Mol. Biol.* **148,** 253–272.
16. Chothia, C. & Janin, J. (1981) *Proc. Natl. Acad. Sci. USA* **78,** 4146–4150.
17. Chothia, C. & Janin, J. (1981) *Biochemistry* **21,** 3955–3965.
18. Novotny, J., Bruccoleri, R. & Newell, J. (1984) *J. Mol. Biol.* **177,** 567–573.
19. Berenstein, F. C., Koetzle, T. F., Williams, G. J. B., Meyer, E. F., Jr., Brice, M. D., Rodgers, J. R., Kennard, O., Shimanouchi, T. & Tasumi, M. (1977) *J. Mol. Biol.* **112,** 535–542.
20. Schultz, G. E. & Schirmer, R. H. (1979) *Principles of Protein Structure* (Springer, New York), p. 69.
21. Phillips, D. C., Sternberg, M. J. E., Thornton, J. M. & Wilson, I. A. (1978) *J. Mol. Biol.* **119,** 329–351.
22. McLachlan, A. D. (1979) *J. Mol. Biol.* **128,** 49–79.
23. Arnold, E., Vriend, G., Luo, M., Griffith, J. P., Kamer, G., Erickson, J. W., Johnson, J. E. & Rossmann, M. G. (1987) *Acta Crystallogr. Sect. A* **43,** 346–361.
24. Xia, Z. X., Shamala, N., Bethge, P. H., Lim, L. W., Bellamy, H. D., Xuong, N. H., Lederer, F. & Mathews, F. S. (1987) *Proc. Natl. Acad. Sci. USA* **84,** 2629–2633.
25. Lim, L. W., Shamala, N., Mathews, F. S., Steenkamp, D. J., Hamlin, R. & Xuong, N. (1986) *J. Biol. Chem.* **261,** 15140–15146.